# The mineralocorticoid receptor forms higher order oligomers upon DNA binding

Gregory Fettweis[1], Thomas A. Johnson[1], Brian Almeida-Prieto[2], Diego M. Presman[3], Gordon L. Hager[1,*], Diego Alvarez de la Rosa[1,2,*]

[1]*Laboratory of Receptor Biology and Gene Expression, National Cancer Institute, National Institutes of Health, Bethesda, Maryland 20892-5055, USA;* [2]*Department of Basic Medical Sciences and Institute of Biomedical Technologies, Universidad de La Laguna, La Laguna 38071, Spain;* [3]*Instituto de Fisiología, Biología Molecular y Neurociencias (IFIBYNE), CONICET-Universidad de Buenos Aires, Facultad de Ciencias Exactas y Naturales, Buenos Aires C1428EGA, Argentina.*

*, corresponding authors: G.L.H., hagerg@dce41.nci.nih.gov; D.A.d.l.R., dalrosa@ull.edu.es

**KEYWORDS**: mineralocorticoid receptor, glucocorticoid receptor, aldosterone, heteromerization, Number & Brightness.

**Short title:** MR and GR adopt different quaternary structures

**Keywords:** mineralocorticoid receptor, glucocorticoid receptor, aldosterone, corticosterone, oligomerization.

## ABSTRACT

The mineralocorticoid and glucocorticoid receptors (MR and GR) are evolutionary related nuclear receptors with highly conserved DNA- and ligand-binding domains (DBD and LBD), which determine promiscuous activation by corticosteroid hormones (aldosterone and glucocorticoids) and binding to a shared DNA consensus sequence, the hormone response element (HRE). In addition, MR and GR functionally interact, likely through direct formation of heteromeric complexes, potentially contributing to cell-specific corticosteroid signaling. It has recently been proposed that agonist and DNA binding promote GR self-association in tetramers. Here we investigated MR quaternary arrangement after receptor activation. To that end we used a fluorescence imaging technique, Number & Brightness (N&B) analysis, in a cell system where receptor-DNA interaction can be studied in live cells in real time. Our results show that agonist-bound MR is a tetramer in the nucleoplasm, forming higher order oligomers upon binding to HREs. Antagonists form intermediate quaternary arrangements, suggesting that the formation of large oligomeric complexes is essential for function. We also show that divergence between MR and GR quaternary arrangements are driven by different functionality of multimerization interfaces in the DBD and LBD and their interplay with the N-terminal domain. In spite of contrasting quaternary structures, MR and GR are able to form heteromers. Given the importance of both receptors as pharmacological targets and the differential oligomerization induced by antagonists, our findings suggest that influencing quaternary structure may be important to provide selective modulation of corticosteroid signaling.

## INTRODUCTION

The mineralocorticoid and glucocorticoid receptors (MR and GR, respectively) are members of the steroid hormone receptor subfamily of nuclear receptors (NR3C). Steroid receptors share a common modular protein architecture (1) that includes a highly-divergent N-terminal domain (NTD), a highly conserved DNA-binding domain and a moderately conserved ligand-binding domain (DBD and LBD) (2). The NTD of both MR and GR is intrinsically disordered but both contain divergent ligand-independent transcription activation function 1 domains (AF-1), that provide an interaction surface for a diversity of transcriptional co-regulators (2-5). The highly conserved DBD between MR and GR imparts essentially indistinguishable DNA binding specificity (6). The LBD similarity between both receptors confers promiscuous ligand activation for MR, binding both mineralocorticoids such as aldosterone or glucocorticoids such as cortisol or corticosterone with similar high affinity (7-10). MR and GR evolved from a gene duplication event predating the appearance of aldosterone (11). MR was then co-opted as a receptor system for a new class of steroid hormones, mineralocorticoids, which regulate mineral and water homeostasis (12). However, MR retained its high-affinity glucocorticoid binding and thus participates in mediating biological responses to both types of hormones (2, 13). Thus, MR and GR have distinct but overlapping physiological functions. Inappropriate activation of MR may mimic or counteract GR actions, promoting obesity and metabolic syndrome (14, 15), enhancing inflammation and tissue fibrosis (16) or diminishing it (17) in a tissue-specific fashion (13), or modulating brain responses to stress (18). MR inhibitors, initially used to treat conditions derived from hyperaldosteronism and situations with excessive water retention have increasingly attracted interest as anti-inflammatory and anti-fibrotic targets (19, 20), with important applications to treat cardiovascular disease (21). In addition to functional crosstalk between MR and GR, there is considerable evidence pointing towards physical interaction and two-way transcriptional modulation between both receptors (17, 22-28).

Growing interest in the molecular basis of specific MR and GR action and the functional role of their physical interaction make it essential to understand the active conformations of both receptors. The prevailing model of dimers as the final active conformation of steroid receptors has been challenged in the past few years (29-32). Using the Number & Brightness (N&B) assay (33) to measure average oligomer size with high spatial resolution in living cells, we have previously reported that agonist-bound GR adopts a dimeric conformation in the nucleoplasm, where the majority of the receptor is soluble, indicating that dimerization precedes high-affinity DNA binding (31, 34). Observation of fluorescently-tagged GR at an array of mouse mammary tumor virus (MMTV) long terminal repeats, containing multiple HRE elements, suggested that the receptor adopts a tetrameric organization upon DNA binding (31). The progesterone receptor (PR) adopts a tetrameric conformation regardless of the nuclear compartment, while the androgen receptor (AR) forms larger oligomeric complexes, with an average of 6 subunits in all nuclear compartments. This paradigm shift in steroid receptor quaternary organization (32, 35) and the close evolutionary relationship of GR with MR, in addition to the formation of heterocomplexes between both receptors, bring forward the question of whether MR and GR share a common quaternary structure. In this study, we used the N&B technique to examine MR oligomerization upon ligand binding. We show striking differences between MR and GR, with MR adopting a tetrameric conformation in the nucleoplasm and forming higher order oligomers upon HRE binding. Known or proposed dimerization interfaces conserved between MR and GR have distinct properties in both receptors. In spite of these differences, GR is able to displace MR subunits and incorporate to heterocomplexes. Our results suggest that modulation of quaternary conformation may be an important parameter to take into consideration during development of selective corticosteroid signaling modulators.

## RESULTS

### Agonist-bound MR forms large oligomers at hormone response elements

MR quaternary structure was investigated in a cell derived from murine C127 adenocarcinoma cell line incorporating in their genome a tandem gene array of approximately 200 copies of the mouse mammary tumor virus promoter (MMTV array), which contain hormone response elements (HREs) (36). This cell line was further modified using CRISPR/Cas9 to knockout the endogenous expression of GR, as previously described (30). Therefore, cells transiently transfected with eGFP-tagged MR allow visualization of the receptor in the nucleoplasm and also enriched at a specific nuclear domain (MMTV array), in the absence of any endogenous GR or MR expression. MR oligomerization was studied using number & brightness (N&B) analysis, a technique that has previously been used to study oligomerization of GR and other steroid receptors in live cells (31, 34). N&B estimates the molecular brightness (ε) of a fluorophore using the first (mean) and second (variance) moments of the intensity fluctuations observed on each pixel of a raster-scan image (33). This way, one can obtained the weighted- average brightness (i.e. oligomeric state) of a protein in the entire nucleus or at a specific region such as the MMTV array. As monomeric and dimeric standards, all experiments included a condition with expression of GR truncated after amino acid 525 (GR-N525), which has been shown to exist in monomeric form in the nucleoplasm and to form dimers in the MMTV gene array (31). This allowed us to normalize every experiment and calculate MR oligomerization relative to this mutant. Unstimulated cells show partial localization of MR to the nucleus (Fig. 1A), as previously described (37, 38). Upon treatment with hormone agonists (either aldosterone or corticosterone), MR fully translocated to the nucleus and produces a bright focus at the MMTV array (Fig. 1A, arrows) (36). N&B analysis showed that unstimulated nuclear MR exists as a monomer (ε = 0.96), but reaches an ε of approximately 4 (4.39; Fig. 1B) upon stimulation with a saturating concentration of aldosterone (10 nM), suggesting the formation of a tetramer in the nucleoplasm. N&B analysis of stably integrated MR also provided an ε near 4, indicating that tetramerization is not an artifact due to transient overexpression (supplementary Fig. S1A). Remarkably, MR concentrated at the MMTV array produces an even higher ε, which approaches 7 (6.92; Fig. 1B), suggesting that higher order oligomerization of MR correlates with chromatin binding and transcriptionally active HREs.

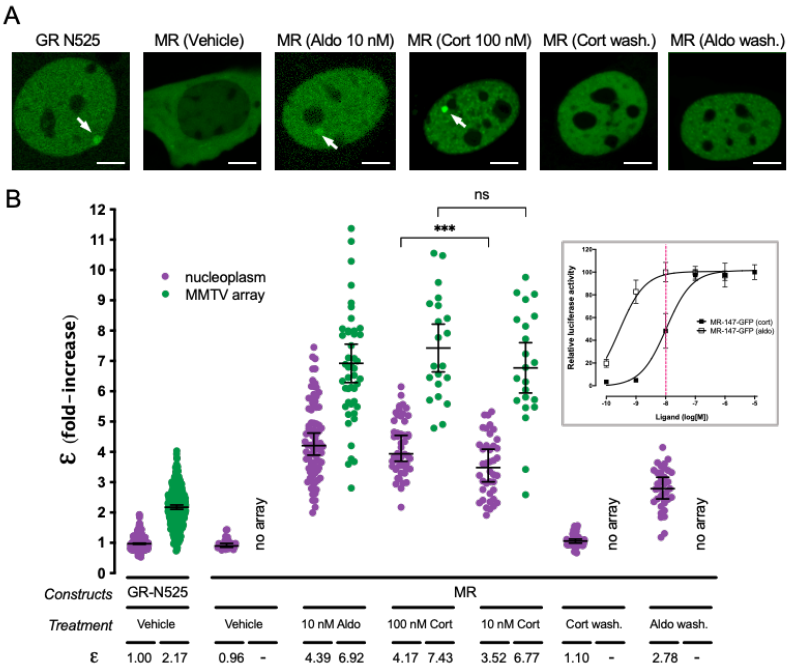

**Figure 1. Agonist-bound MR adopts a tetramer conformation in the nucleoplasm and forms higher order oligomers at HREs**. (A) Representative images of single cell nuclei expressing GFP-GR-N525 or MR-GFP and treated with vehicle, 10 nM aldosterone (Aldo) or 100 nM corticosterone (Cort). In certain experiments, agonists were washed out after one hour stimulation (wash.). White arrows point to the MMTV array. Scale bars: 5 µm. (B) Normalized molecular brightness (ε). Each point represents a single nucleus (n = 490, 307, 26, 82, 47, 50, 21, 40, 22, 55, 36 cells in each condition, from left to right). Horizontal bars represent mean ± 95% confidence interval (CI). Wash., washout. Statistical analysis was performed using one-way ANOVA followed by Tukey test (results are shown only for two selected pairs; ***, $p < 0.001$; n.s., not significant). Inset, MR dose-response gene transactivation curves in response to aldosterone (aldo) and corticosterone (cort). Curves were obtained using wild-type mouse MR transiently transfected in COS7 cells co-expressing a luciferase gene reporter system and treated with the indicated concentrations of hormones for 16h. Dashed red line highlights the difference in MR activity at 10 nM hormone concentration (data adapted from (23)).

Since both aldosterone and glucocorticoids are endogenous agonists of MR, we tested whether receptor oligomerization varies as a function of the agonist. To that end, we compared the results obtained with aldosterone to those obtained with saturating concentrations of corticosterone (Cort, 100 nM), a dose that produces full receptor activation (Fig. 1B, inset). Our results show that both agonists produce indistinguishable ε values that are consistent with a tetrameric organization in the nucleoplasm and a higher order oligomer in the MMTV array (Fig. 1A and 1B). In order to further test the relationship between agonist binding and oligomerization, we took advantage of an important difference between aldosterone and corticosterone. Both hormones bind MR with equal high affinity ($K_d$ ~ 0.5 nM), but aldosterone is more effective in activating the receptor ($EC_{50}$[aldo] = 0.5 nM vs. $EC_{50}$[cort] = 10 nM). This difference in potency has been ascribed to a higher off-rate of glucocorticoids in the receptor (39). Therefore, we tested a lower concentration of corticosterone (10 nM), which fully saturates the receptor but produces 50% of the maximum activity (Fig. 1B, inset, vertical dashed line). Under those conditions, nucleoplasmic MR showed a statistically significant lower ε value (ε = 3.52; Fig. 1B), suggesting a correlation between hormone off-rate and oligomerization. In contrast, MR in the MMTV array still showed a high value (ε = 7), which is consistent with required ligand binding for high-affinity interaction with HREs (40).

We next studied the reversibility of agonist-induced oligomerization of MR. To that end cells were incubated with agonists for 1 hour, followed by hormone washout and an additional 4-hour incubation before recording. Under those conditions, MR still showed full nuclear localization (i.e., negligible nuclear export), but no binding to the MMTV array (Fig. 1A). N&B analysis revealed that after corticosterone washout MR reverted to a monomeric organization in the nucleoplasm (Fig. 1B). In contrast, aldosterone washout produced incomplete reversal, with a nucleoplasmic MR ε value of 2.8 (Fig. 1B), suggesting a mixed population of tetramers with dimers and/or monomers. This could be explained by the shorter off-rate of aldosterone binding to the receptor (39). These results demonstrate that higher order oligomerization depends on agonist binding in a reversible manner.

**Antagonists induce intermediate-size MR oligomers**

Clinically relevant MR antagonists such as spironolactone or eplerenone induce nuclear translocation, although with slower kinetics (37, 41, 42). We asked whether these antagonists also facilitate MR binding to HREs and what is the quaternary structure of the receptor under these conditions. Our results showed that both spironolactone and eplerenone induced MR binding to the MTTV array (Fig. 2). However, N&B revealed that MR oligomerization in the nucleoplasm and in the MMTV array does not reach the levels detected with agonists. Remarkably, there are clear differences between both antagonists. Spironolactone produced an ε value of 2.04 in the nucleoplasm, consistent with a population mainly form by MR dimers, and 4.43 at the MMTV array, consistent with

tetramerization upon HRE binding (Fig. 2). In contrast, eplerenone showed lower ε, even at high antagonist concentration, with predominantly monomeric MR in the nucleoplasm (ε = 1.02-1.36, similar to the unstimulated receptor) and an ε of 2.31-2.75 at the MMTV array (Fig. 2). These results suggest that the high-order oligomerization detected with saturating concentrations of agonists represent the fully active conformation of MR, while different antagonists produce intermediate steps in the building of the fully active oligomer.

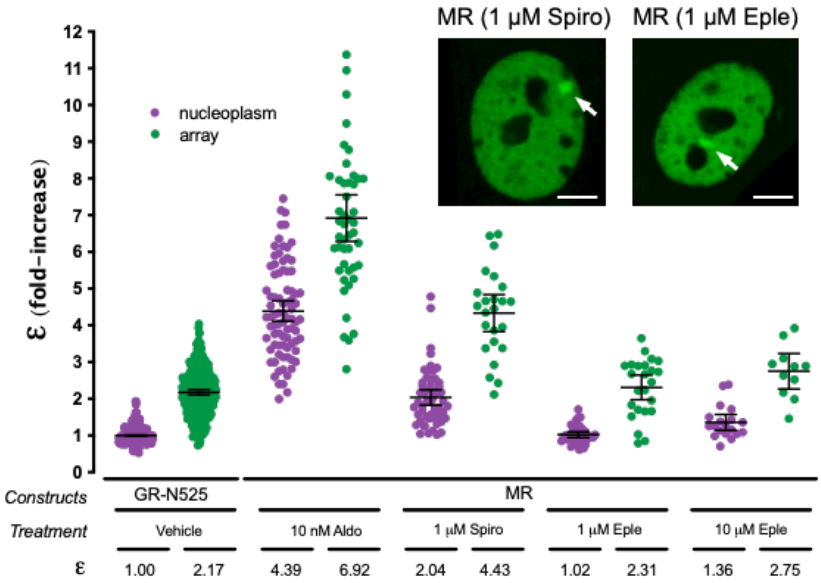


**Figure 2. MR antagonists produce different MR quaternary configurations**. (A) Representative images of single cell nuclei expressing MR-GFP and treated with 1 μM spironolactone (Spiro) or 1 μM eplerenone (Eple). White arrows point to the MMTV array. Scale bars: 5 μm. (B) MR molecular brightness (ε) assessed using the N&B technique. To facilitate comparison, data from Fig.1 showing ε for GR-N525 and MR treated with 10 nM aldosterone are included. Data points correspond to ε obtained from a single nucleus (n = 490, 307, 82, 47, 55, 24, 37, 24, 19 and 11 cells in each condition, from left to right). Horizontal bars represent mean ± 95% CI.

## MR and GR do not share the same dimerization interfaces

MR and GR evolved from a common corticoid receptor through gene duplication (11, 43) and have high sequence conservation in the DBD (94% identity) and moderate conservation in the LBD (57% identity; supplementary Fig. S2). Both domains harbor key determinants for GR oligomerization (31). The results described above uncover a profound difference between ligand-bound GR and MR quaternary conformation in the nucleus, probably reflecting different functionalities of the oligomerization interfaces between both receptors. To test this hypothesis, we analyzed the role of key residues in DBD and LBD in the process (Fig. 3A and 3B). To directly test the role of DNA binding, we first introduced the mutation C603S, which completely disrupts the first zinc finger in the DBD (Fig. 3A), eliminating the possibility of DNA binding (44, 45). This mutation produced a receptor that was unable to bind the MMTV array (Fig. 3C) and exists as a monomer in the nucleoplasm (Fig. 3D), suggesting that the effect of disrupting the P-loop is likely not limited to preventing DNA binding but has additional effects on the structure of the receptor.

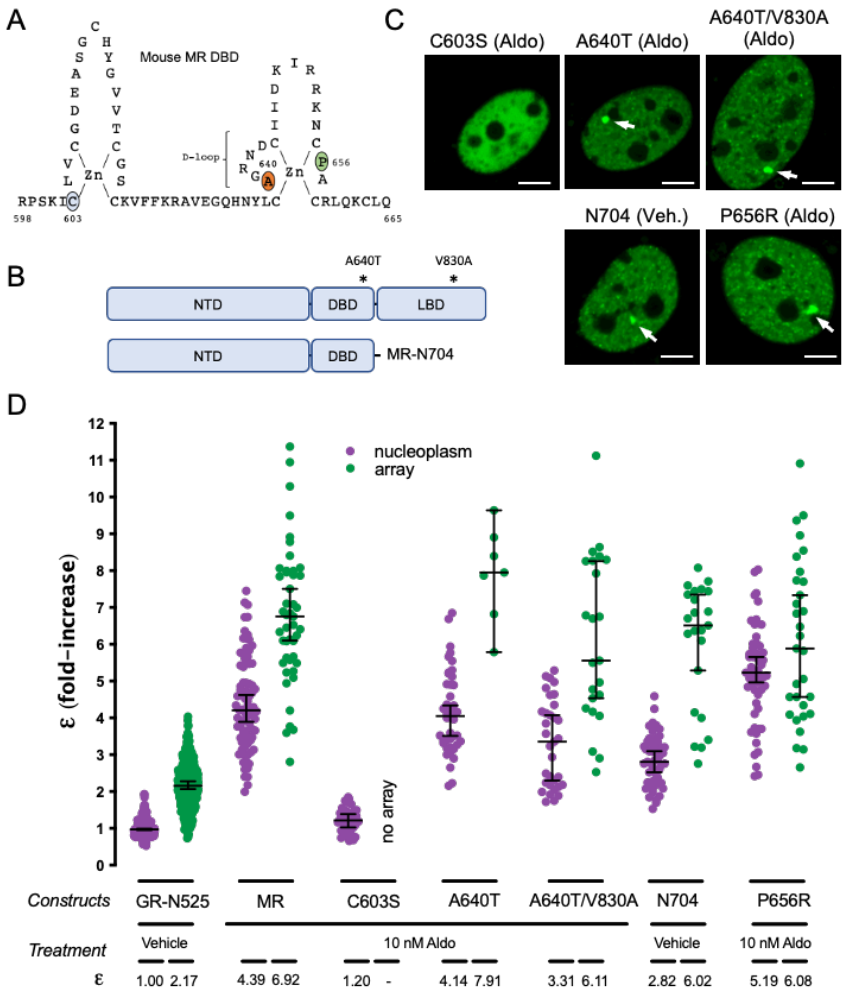


**Figure 3. The role of predicted MR dimerization interfaces in quaternary structure formation.** (A) Schematic representation of MR DBD. (B) Schematic representation of MR double mutant (A640T/V830A) and deletion generating construct MR-N704. NTD, N-terminal domain; DBD, DNA binding domain; LBD, ligand binding domain. (C) Representative images of single cell nuclei expressing the indicated constructs. White arrows point to the MMTV array. Scale bars: 5 µm. (D) MR molecular brightness (ε) assessed using the N&B technique. To facilitate comparison, data from Fig.1 showing ε for GR-N525 and MR treated with 10 nM aldosterone are included. Data points correspond to ε obtained from a single nucleus (n = 490, 307, 82, 47, 41, 44, 7, 33, 23, 51, 23, 57 and 31 cells in each condition, from left to right). To facilitate comparison, data from Fig.1 showing ε for GR-N525 and MR treated with 10 nM aldosterone are included. Horizontal bars represent mean ± 95% CI.

The DBD of GR contains a 5 amino acid sequence, the D-loop (supplementary Fig. S2) that has been proposed to be critical for dimerization (46). Mutation A465T in the D-loop of GR, commonly known as GRdim, was originally proposed to prevent DNA binding and dimerization of GR, although later work has shown that GRdim still forms dimers (34, 47), although its activity as transcriptional modulator is severely weakened (48). Combination of A465T mutation with an additional mutation in the LBD (I634A) does produce a monomeric GR (GRmon; (31, 34, 49)). In the case of MR, the orthologous mutation equivalent to GRdim (A640T; Fig. 3A; supplementary Fig. S2) did not produce any effect on receptor oligomerization in the nucleoplasm or the MMTV array (Fig. 3D). The combination of point mutations A640T/V830A, equivalent to the double mutant A465T/I634A in GRmon, reduced values to 3.31 in the nucleoplasm and 6.11 in the array (Fig. 3D), indicating that the function of these two well-

described dimerization interfaces in GR is only partially conserved in MR, with a minor role in configuring its quaternary structure. To further test this idea, we deleted the whole LBD by truncating MR after amino acid 704 (MR-N704; Fig. 3B). MR-N704 is constitutively nuclear and binds the array in the absence of ligand (Fig. 3C), as described previously for the equivalent GR deletion, GR-N525 (31). MR-N704 produced reduced ε values in the nucleoplasm (2.8) and in the MMTV array (6) compared to the WT receptor (Fig. 3D), similarly to the A640T/V830A mutant. This stands in contrast to the equivalent deletion in GR, which produces monomers in the nucleoplasm and dimers at the MMTV array (Fig. 1; (31)), further indicating that the functionality of the classic GR dimerization interfaces is not fully conserved on MR.

To continue probing the role of the DBD and LBD dimerization interfaces, we introduced the mutation MR-P654R in the D-loop of the DBD (Fig. 3A), located in a residue that is fully conserved in GR (supplementary Fig. S2), where it mimics DNA binding, resulting in tetrameric receptors in the nucleoplasm with significantly enhanced activity (30). N&B results showed that mutant MR-P654R shows a higher order oligomerization status in the nucleoplasm (ε = 5.19; Fig. 3D), approaching the value found at the array, although the effect is not as stark as the one found with GR (31). The activity of MR-P654R on enhancing the expression of well-known MR/GR target genes such as *Per1*, *Sgk1* or *Serpine1* was not significantly different from the WT construct (supplementary Fig. S3), similarly to the effect of the equivalent mutation in GR, which does not significantly change the potency of the receptor but rather expands its set of target genes (30).

**The NTD participates in MR tetramer formation in the nucleoplasm**

Altogether, our analysis of highly conserved residues in the DBD and LBD of MR and GR that have been involved in GR dimerization indicates that their impact on MR is significantly lower, pointing to the involvement of other regions of the receptor in the formation of its quaternary structure. Given that the NTD shows low sequence conservation between MR and GR (<15% identity), we first deleted this entire domain, generating a truncated MR with the last 580 amino acids of the sequence (MR-580C, Fig. 4A). This construct showed an ε value of 1.6 in the nucleoplasm, indicating its essential role in ligand-induced, HRE-independent tetramerization of MR (Fig. 4B). Interestingly, this construct binds to the MMTV array (Fig. 4B), where it still forms higher order oligomers (ε = 6.6), almost indistinguishable from the wild type MR. This result suggests that tetramerization in the nucleoplasm is not a pre-requisite to form higher order oligomers in the MMTV array and also that MR DBD and LBD contain oligomerization interfaces that are triggered by HRE binding. Swapping the NTD of MR for the equivalent domain in GR (construct GR-N408/MR-580C, Fig. 4A) produced an intermediate oligomer size in the nucleoplasm (ε = 3.0, Fig. 4C), further confirming that ligand-induced tetramerization of MR necessitates both its NTD and LBD. This construct behaves almost normally in the MMTV array (ε = 6.4, Fig. 4C), again pointing to the importance of the DBD in higher order oligomerization. We also performed the opposite swap, creating a construct with the NTD of MR and DBD and LBD from GR (construct MR-N579/ GR-407C, Fig. 4A). Since aldosterone binds with lower affinity (Kd = 14 nM) and is a very poor activator of GR, we used 100 nM dexamethasone to stimulate this construct (31). The MR-N579/ GR-407C chimera produced an intermediate oligomer in the nucleoplasm (ε = 2.57), but still higher order quaternary organization in the MMTV array (ε = 7.89; Fig. 4C).

Taken together, our data suggest the possibility that MR has additional oligomerization determinants in the NTD. To further investigate this possibility, we generated a construct with deletion 382-510 (MR-Δ382-510 (Fig. 4A), which eliminates a region that has been previously implicated in a

ligand-dependent N/C interaction in MR (50), and should also disrupt the second part of the bi-partite activator function-1 domain (AF-1b; (3, 5)). Remarkably, this deletion did not affect nucleoplasm tetramerization but clearly diminished oligomer size at the array (Fig. 4C), implicating this region in the formation of the final active conformation of MR.

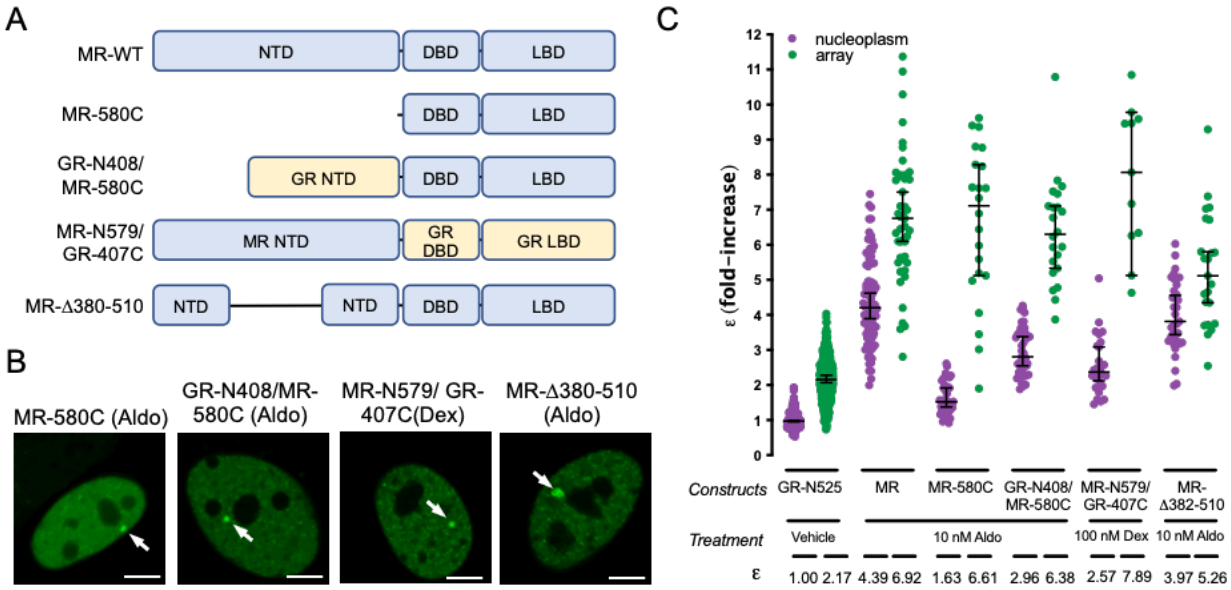


**Figure 4. The NTD is essential for MR tetramerization in the nucleoplasm.** (A) Schematic representation of MR deletion and domain swapping constructs. NTD, N-terminal domain; DBD, DNA binding domain; LBD, ligand binding domain. (B) Representative images of single cell nuclei expressing the indicated constructs. White arrows point to the MMTV array. Scale bars: 5 µm. (C) N&B results obtained with the indicated constructs. To facilitate comparison, data from Fig.1 showing ε for GR-N525 and MR treated with 10 nM aldosterone are included. Data points correspond to ε obtained from a single nucleus (n = 490, 307, 82, 47, 42, 22, 43, 22, 35 and 23 cells in each condition, from left to right). Horizontal bars represent mean ± 95% CI.

### GR is able to incorporate into GR-MR heteromers, displacing MR subunits

GR and MR physically interact (17, 23-28), and their co-expression likely results in the modulation of both of their transcriptional programs (17, 22-24, 27, 28). The differences in quaternary organization between MR and GR raise an additional question. Would co-expressed MR and GR adopt a GR-like tetrameric conformation, an MR-like higher order oligomerization or a combination of both? To address this question, we performed N&B experiments in cells co-transfected with both receptors, eGFP-tagged MR with mCherry-tagged GR, recording data on the eGFP channel only. If GR incorporates into MR complexes, displacing some MR subunits, then MR's ε value should drop in the presence of GR. On the contrary, if GR adds up to MR, then ε values should remain the same. Imaging of transfected cells showed that co-expression of both receptors produced simultaneous occupancy of the MMTV array (Fig. 5A). Interestingly, GR co-expression significantly reduced ε for MR, both in the nucleoplasm and in the array (Fig. 5B). Surprisingly, co-binding of both receptors to the MMTV array and the effect of GR lowering the apparent ε for MR occurred even when aldosterone was used as an agonist (Fig. 5A and 5B). It is worth noting that even though aldosterone does not activate GR at the concentration used in these experiments (10 nM), it does at least partially occupy the receptor (Kd = 14 nM; (51)), as evidenced by its nuclear translocation and binding to the MMTV array even in the absence of MR (ε =

1.35 in the nucleoplasm and 2.15 in the MMTV array; supplementary Fig. S1B). Since these experiments use transiently transfected cells, the effect of co-expressing competing GR would be expected to vary depending on the relative proportion of MR and GR expressed in the cell. Therefore, we measured the ratio of eGFP and mCherry intensities in each cell after each N&B recording and plotted it against ε, obtaining a positive correlation between both parameters (Fig. 5C). In conclusion, our data indicates that GR and MR can form heterocomplexes in live cells, wherein GR can displace some MR subunits, rendering a complex stoichiometry that requires further study.

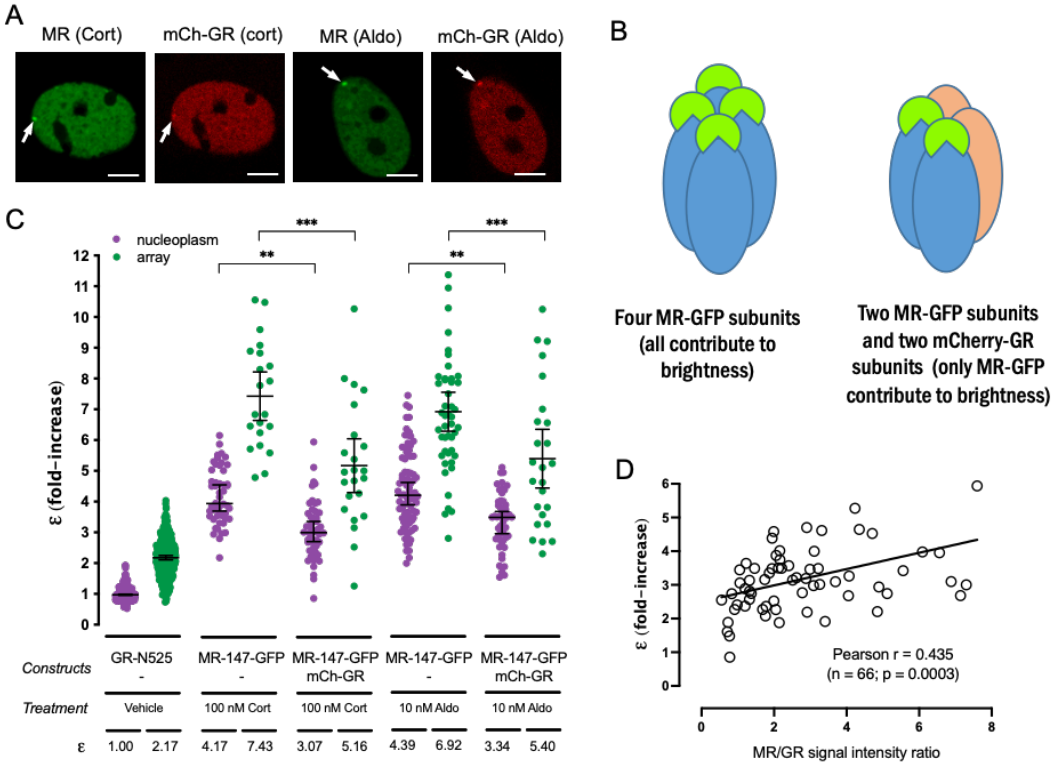


**Figure 5. GR displaces MR subunits from the oligomer**. (A) Representative images of single cell nuclei expressing the indicated constructs. mCh, mCherry. White arrows point to the MMTV array. Scale bars: 5 µm. (B) MR molecular brightness (ε) assessed using the N&B technique. To facilitate comparison, data from Fig.1 showing ε for GR-N525 and MR treated with 100 nM corticosterone or 10 nM aldosterone are included. Data points correspond to ε obtained from a single nucleus (n = 490, 307, 50, 21, 50, 23, 82, 47, 50 and 25 cells in each condition, from left to right). Statistical analysis was performed using one-way ANOVA followed by Tukey test (results are shown only for two selected pairs; *, $p < 0.05$; **, $p < 0.01$; $p < 0.001$). (C) Linear correlation between eGFP-MR ε values and the ratio of MR/GR fluorescence intensity. Each dot represents an individual nucleus. Pearson lineal correlation coefficient was computed using Prism 9 (GraphPad).

## DISCUSSION

### Evolutionary conservation of quaternary structure and its impact for heteromerization

Here we used the N&B fluorescence imaging technique on living cells to study MR quaternary structure and its changes upon ligand binding and high-affinity interaction with HREs. Our results support a unique oligomeric conformation among the steroid receptor subfamily, with results compatible with tetramer formation induced by agonist binding, which generates larger oligomers after

binding to specific sites in the DNA. This stands in contrast to the quaternary structure of GR (31), the closest relative of MR within the subfamily. It may be assumed that protein divergence during evolution is constrained by selective pressure to maintain protein structure, including stable protein-protein interactions forming quaternary arrangements (52, 53). It follows that proteins with closely related evolutionary origin and functions would be expected to share the same quaternary arrangement. Proteins that share very high sequence identity (> 90%), quaternary structure is almost always conserved (54). However, proteins showing more moderate sequence identity tend to differ more in their quaternary structures. Indeed, it has been calculated that 30-40% identity correlates with a 70% probability of sharing a quaternary structure (55). For instance, the NSAR/OSBS subfamily of enzymes presents overall sequence identity > 40%, but some of its members are dimers and some octamers (56). It is also worth noting that the final quaternary structure of proteins might be underestimate due to bias in the techniques used to determine oligomeric states (57). Sequence conservation between MR and GR, and in general between steroid receptors, differs significantly between domains, with low conservation in the NTD (less than 15% identity), medium conservation in the LBD (approx. 60%) and highly conserved DBD (94% identity). Given the very low conservation in the NTD, which our data suggests plays an important role in oligomer formation, and the medium sequence identity in the LBD, which should also play a role, it is not altogether surprising that MR and GR adopt different quaternary structures.

It has long been known that nuclear receptors in the NR1 subfamily function by forming heteromers with RXR (58). However, it is increasingly clear that NR3 receptors are also able to form so-called “atypical” heteromers, which include NR3 interactions with NR1 receptors, as well as RXR (58). In addition, NR3 receptors form heteromers with members of the same subfamily. These include not only MR-GR interactions, but others such as GR association with PR, ER or AR (58, 59), or MR interaction with ER (60), just to name a few (58). Taken together, this suggests that nuclear receptor crosstalk frequently involves formation of heteromers and that this is not hampered by the different quaternary conformations adopted by homomers, as confirmed by our data. This direct interaction model does not necessary implicate direct binding of both kind of receptors to DNA, but may also involve tethering, looping or simply sequestration of one receptor by the other, preventing its genomic action. In the case of MR-GR interaction, it appears that they exert reciprocal effects on each other. It has recently been shown that MR modulates GR response to a synthetic glucocorticoid in mouse keratinocytes (22). In general, co-expression of MR and GR has been shown to alter glucocorticoid responses, although these effects appear to be cell-type and promoter-specific (24, 27, 28, 61-63). In addition, it is difficult to tease out whether transcriptional responses are primarily driven by GR, by MR or both. It has also been proposed that MR may exert its effects not directly binding to DNA, but through tethering to GR (27). There are few reports examining the role of GR on MR/Aldo function. Tsugita et al. used gene-reporter assays to show that GR co-expression is necessary for MR function, in a process likely involving receptor heteromerization and DNA binding (64), a model that we have recently confirmed investigating MR genome-wide binding and Aldo-regulated transcriptome (Johnson et al., *BIORXIV/2023/525745*). It has recently been reported that abnormally high oligomeric forms of GR at the MMTV array, such as D647V that causes Chrousos disease, correlates with less transcriptional activity (29). In this sense, it is tempting to speculate that MR’s higher oligomeric conformation is not optimal, and thus GR might increase MR activity (Johnson et al., *BIORXIV/2023/525745;* (28, 62, 64)) by reducing its stoichiometry. Nevertheless, whether the different reciprocal actions of MR and GR on their transcriptional activity reflect differences in the quaternary structure of the heterocomplexes requires further investigation.

**Mechanisms of oligomer formation**

Results comparing binding of antagonists and agonists indicate that different ligands promote different average quaternary structures in the receptor population. Spironolactone and eplerenone produced oligomers that are roughly multiples of two (Fig. 2), In fact, it is thought that an energetically-favorable, ordered pathway underlies formation of most protein complexes, although multiple parallel pathways are also possible (54). Also, the subcomplexes formed during assembly of larger oligomers appear to correlate with evolutionary precursors (65). It has been proposed that comparing homologous proteins with differing quaternary structures, such as the NR3 family of steroid receptors ((31) and the results presented here) can trace the evolution of a homomeric complex (55, 66). Thus, it is tempting to speculate that building the final active conformation of MR involves an initial dimerization of soluble subunits upon ligand binding, possibly common to all steroid receptors, followed by stepwise doubling of oligomer size, which also appears to take place in other NR3 receptors, such as PR (31). The fact that the most potent agonist, aldosterone, does not generate an average oligomer size of 8, but reaches an average of 7, suggests that the population being observed could be an uneven combination of tetramers and octamers, with predominant presence of the latter.

Inter-subunit interfaces mediating the different steps in forming MR tetramers or higher order oligomers remain to be studied in detail. Our data indicates that all three domains (NTD, DBD and LBD) appear to play a role, with complex interactions between them. In general, it appears that each domain has a modest contribution on its own, as reflected by small decreases in $\varepsilon$ when they are disrupted by deletion of point mutations in known GR dimerization interfaces. The only exception is mutation C603S, which completely disrupts the first zinc-finger domain in the DBD. This mutation renders MR monomeric and unable to bind DNA (44, 45). However, it is not possible to infer that the DBD is the essential domain for DNA oligomerization, since the impact of this mutation on the structure of the receptor may be wider and also, it precludes DNA binding and possibly allosteric interactions between the DBD and LBD, proposed to play an important role in GR tetramerization (31, 32).

**Functional impact of oligomerization**

The correlation between agonist and antagonist binding and the size of the MR oligomer strongly suggests that higher order oligomerization detected only after agonist and DNA binding represents an active conformation of the receptor. However, our data does not shed light directly on the functional impact of MR oligomerization, particularly in the implications of higher-order oligomer formation upon binding to HREs. GR modulation on MR stoichiometry is certainly intriguing. In the case of GR, the “tetra” mutation, P481R, stabilizes the tetrameric conformation of the receptor (31), allowing functional dissection of tetramerization, which has been shown to potently drive chromatin interactions and transcriptional activity (30). The equivalent mutation in MR, P654R, does increase oligomer size in the nucleoplasm from 4.39 to 5.19, but this is a much more modest change that does not appear to change transcriptional regulation of endogenous genes (supplementary Fig. S3). It remains to be examined whether this small increase would produce a genome-wide effect changing MR chromatin binding and/or transcriptional outcomes. Ideally, further investigating the mechanisms of MR oligomer formation will provide tools to stabilize the larger oligomers, making it easier to assess their functional importance.

**Conclusions**

In summary, we have shown that MR adopts a distinct quaternary structure, further supporting a model where each steroid receptor adopts different conformations that are not determined by their

evolutionary relationships. These differences do not appear to preclude formation of heteromeric complexes between NR3C receptors. Large MR oligomers in the MMTV array are reached only with agonists, suggesting a relationship between oligomer size and the final active conformation of the receptor. Structural determinants of MR oligomerization appear complex, with participation of all three main domains. These results have important implications for the pharmacological modulation of steroid receptor signaling.

## MATERIAL AND METHODS

*Plasmids constructs and mutagenesis*

A fully functional mouse MR fluorescent derivative with insertion of enhanced green fluorescent protein (eGFP) after amino acid 147 has been previously described (67). N-terminus eGFP tagged wild type mouse GR or truncated mutant GR-N525, lacking the entire LBD, (eGFP-GR and eGFP-GRN525, respectively) have been previously described (31, 68). A plasmid expressing mouse GR tagged in the N-terminus with mCherry was developed by amplifying mouse GR coding sequence and in-frame cloning in pmCherry-C3 (Clontech). Point mutations and deletions were introduced using the Quickchange XL mutagenesis kit (Agilent) following the manufacturer´s instructions. Domain swapped mouse MR/GR constructs were constructed by amplification of the relevant fragments from donor plasmids and directional cloning using ligation-free In-Fusion technology (Clontech) in PCR-mediated linearized vectors. PCRs were performed using high-fidelity Pfu ultra II polymerase (Agilent). All constructs and mutations were confirmed by DNA sequencing.

*Cell culture, transfection and treatment with ligands*

The cell lines used in this study originally derive from mouse mammary carcinoma cell line C127 (RRID: CVCL_6550), which were originally modified introducing approximately 200 copies of a tandem array of the Harvey viral ras (MMTV-v-Ha-ras) reporter, which contains several HREs (36). This cell line was then modified using CRISPR/Cas9 to knockout the endogenous expression of GR, as previously described (30). When indicated, a cell line with stable integration of a plasmid containing eGFP-MR driven by the CMV promoter was used. This cell line was developed using the CRISPR/Cas9 procedure, as previously described (30). Cells with plasmid insertion were selected by puromycin treatment followed by fluorescence-activated cell sorting (FACS). Since expression of MR in the sorted polyclonal cell population declined over time, we further selected stable lines by single-cell cloning. eGFP-MR expression was confirmed by confocal microscopy previously described (23). All cell lines were grown in Dulbecco's modified Eagle's medium (DMEM), 10% fetal bovine serum (FBS), sodium pyruvate, nonessential amino acids and 2 mM glutamine. Culture medium and reagents were obtained from Gibco, except FBS, which was from Gemini. Culture medium also contained 5 µg/mL tetracycline (Sigma–Aldrich) to prevent expression of a stably integrated eGFP-GR (34). Cells were maintained at 37C and 5% CO2 in a humified incubator. Forty-eight hours before experiments, cells were plated in 2-well borosilicate glass chambers (Nunc™ Lab-Tek™ II, ThermoFisher #155379) in DMEM supplemented with 10% charcoal/dextran-treated FBS (CS-FBS). Next day, cells were transfected using Jetprime (Polyplus) according to the manufacturer´s instructions. On the day of the experiment, cells were treated for 1h with ligands dissolved in ethanol (vehicle) and added to the medium at the final concentration indicated in each experiment. Hormone washout was performed by three consecutive 10-minute washes with prewarmed hormone-free complete medium with CS-FBS, followed by incubation in the same medium for 4h. All ligands were obtained from Sigma-Aldrich.

*Number and brightness (N&B) analysis*

N&B was performed as previously described (31, 34). Briefly, cells were placed in an environmentally controlled chamber in a Zeiss LSM780 confocal microscope and maintained at 37ºC and 5% $CO_2$ throughout the duration of the experiment. After approximately 30 min of equilibration, single nuclei were imaged using a 63X oil immersion objective (N.A. = 1.4). Cells were imaged between 30 min and 2h after addition of each ligand. Fluorescence excitation was performed with a multi-line argon laser tuned at 488 nm and detection was performed with a gallium arsenide phosphide detector set in photon-counting mode. For each nucleus, stacks of 150 images (256 x 256 pixels) from a single plane were taken, using a pixel size of 80 nm and a pixel dwell time of 6.3 µs. Recording conditions ensured sampling of independent populations of molecules (31, 34, 69). Data analysis was performed using Globals for Images · SimFCS 2 software (Laboratory for Fluorescence Dynamics, University of California, Irvine, CA). Pixels were classified as nucleoplasm or MMTV array according to their intensity values. Quality control for analysis followed our previously described guidelines (31, 34). Average fluorescence intensity (<I>) and variance (σ2) were calculated for each pixel along the image stack. The ratio of σ2 to <I> provides the apparent brightness (B). Real brightness (ε) was calculated as B – 1 (31, 34). Each experimental condition was repeated independently two to five times. Results from all experiments were pooled after normalizing with the internal monomeric control (GR-N525**)**. When indicated, mCherry-GR was co-transfected with eGFP-MR and the average intensity of mCherry fluorescence was recorded for the nucleus of interest before performing the N&B experiment.

*RNA Isolation, qPCR and RNA-seq analysis*

Cells cultured for at least 24h on CS-FBS supplemented culture medium were treated with vehicle, 10 nM aldosterone or 100 nM corticosterone for 2 h. Total RNA was purified using a commercially available kit (Macherey-Nagel NucleoSpin RNA isolation) that includes an in-column DNase digestion step. Purified RNA was quantified using spectrophotometry and frozen at -80ºC. Single-stranded cDNA was synthesized from 1 µg of total RNA as template using a commercially available kit (iScript cDNA Synthesis Kit, Biorad). RT-qPCR analysis of nascent mRNA abundance was performed in duplicate using iQ SYBR Green Supermix (Biorad #1708880) in a Biorad CFX96 machine. Primers for the amplification of nascent Per1, Sgk1 and Serpine1 were as described (48).

## ACKNOWLEDGMENTS

This research was supported by the Intramural Research Program of the NIH, National Cancer Institute, Center for Cancer Research. DAdlR was supported by grants PID2019-105339RB-I00 (funded by MCIN/AEI/10.13039/501100011033 and “ERDF A way of making Europe”), and PRX18/00498 (funded by *Programa Estatal de Promoción del Talento y su Empleabilidad en I+D+i, Subprograma Estatal de Movilidad, del Plan Estatal de I+D+I,* MICINN, Spain). BA-P was supported by pre-doctoral fellowship BES-2017-082939 (funded by MCIN/AEI/ 10.13039/501100011033 and by “ESF Investing in your future”). D.M.P. was supported by CONICET and the Agencia Nacional de Programación Científica y Tecnológica [PICT 2019-0397 and PICT 2018-0573].

## REFERENCES


1. S. Green, P. Chambon, Oestradiol induction of a glucocorticoid-responsive gene by a chimaeric receptor. *Nature* **325**, 75-78 (1987).
2. C. Grossmann, B. Almeida-Prieto, A. Nolze, D. Alvarez de la Rosa, Structural and molecular determinants of mineralocorticoid receptor signalling. *Br J Pharmacol* **179**, 3103-3118 (2022).
3. H. Fuse, H. Kitagawa, S. Kato, Characterization of transactivational property and coactivator mediation of rat mineralocorticoid receptor activation function-1 (AF-1). *Mol Endocrinol* **14**, 889-899 (2000).
4. D. N. Lavery, I. J. McEwan, Structure and function of steroid receptor AF1 transactivation domains: induction of active conformations. *Biochem J* **391**, 449-464 (2005).
5. L. P. Tallec *et al.*, Protein inhibitor of activated signal transducer and activator of transcription 1 interacts with the N-terminal domain of mineralocorticoid receptor and represses its transcriptional activity: implication of small ubiquitin-related modifier 1 modification. *Mol Endocrinol* **17**, 2529-2542 (2003).
6. W. H. Hudson, C. Youn, E. A. Ortlund, Crystal structure of the mineralocorticoid receptor DNA binding domain in complex with DNA. *PLoS One* **9**, e107000 (2014).
7. J. L. Arriza *et al.*, Cloning of human mineralocorticoid receptor complementary DNA: structural and functional kinship with the glucocorticoid receptor. *Science* **237**, 268-275 (1987).
8. R. K. Bledsoe *et al.*, Crystal structure of the glucocorticoid receptor ligand binding domain reveals a novel mode of receptor dimerization and coactivator recognition. *Cell* **110**, 93-105 (2002).
9. J. Fagart *et al.*, Crystal structure of a mutant mineralocorticoid receptor responsible for hypertension. *Nat Struct Mol Biol* **12**, 554-555 (2005).
10. Y. Li, K. Suino, J. Daugherty, H. E. Xu, Structural and biochemical mechanisms for the specificity of hormone binding and coactivator assembly by mineralocorticoid receptor. *Mol Cell* **19**, 367-380 (2005).
11. M. E. Baker, Y. Katsu, Evolution of the Mineralocorticoid Receptor. *Vitam Horm* **109**, 17-36 (2019).
12. B. C. Rossier, M. E. Baker, R. A. Studer, Epithelial sodium transport and its control by aldosterone: the story of our internal environment revisited. *Physiol Rev* **95**, 297-340 (2015).
13. E. Gomez-Sanchez, C. E. Gomez-Sanchez, The multifaceted mineralocorticoid receptor. *Compr Physiol* **4**, 965-994 (2014).
14. F. Fallo *et al.*, Prevalence and characteristics of the metabolic syndrome in primary aldosteronism. *J Clin Endocrinol Metab* **91**, 454-459 (2006).
15. B. Schreier, A. Zipprich, H. Uhlenhaut, M. Gekle, Mineralocorticoid receptors in non-alcoholic fatty liver disease. *Br J Pharmacol* **179**, 3165-3177 (2022).
16. C. van der Heijden, M. Bode, N. P. Riksen, U. O. Wenzel, The role of the mineralocorticoid receptor in immune cells in cardiovascular disease. *Br J Pharmacol* **179**, 3135-3151 (2022).
17. J. Bigas, L. M. Sevilla, E. Carceller, J. Boix, P. Perez, Epidermal glucocorticoid and mineralocorticoid receptors act cooperatively to regulate epidermal development and counteract skin inflammation. *Cell Death Dis* **9**, 588 (2018).
18. S. N. Paul, K. Wingenfeld, C. Otte, O. C. Meijer, Brain mineralocorticoid receptor in health and disease: From molecular signalling to cognitive and emotional function. *Br J Pharmacol* **179**, 3205-3219 (2022).
19. F. Jaisser, N. Farman, Emerging Roles of the Mineralocorticoid Receptor in Pathology: Toward New Paradigms in Clinical Pharmacology. *Pharmacol Rev* **68**, 49-75 (2016).
20. A. Lother, F. Jaisser, U. O. Wenzel, Emerging fields for therapeutic targeting of the aldosterone-mineralocorticoid receptor signaling pathway. *Br J Pharmacol* **179**, 3099-3102 (2022).
21. J. Bauersachs, N. Lopez-Andres, Mineralocorticoid receptor in cardiovascular diseases-Clinical trials and mechanistic insights. *Br J Pharmacol* **179**, 3119-3134 (2022).
22. E. Carceller-Zazo *et al.*, The mineralocorticoid receptor modulates timing and location of genomic binding by glucocorticoid receptor in response to synthetic glucocorticoids in keratinocytes. *FASEB J* **37**, e22709 (2023).
23. R. Jimenez-Canino, M. X. Fernandes, D. Alvarez de la Rosa, Phosphorylation of Mineralocorticoid Receptor Ligand Binding Domain Impairs Receptor Activation and Has a Dominant Negative Effect over Non-phosphorylated Receptors. *J Biol Chem* **291**, 19068-19078 (2016).

24. W. Liu, J. Wang, N. K. Sauter, D. Pearce, Steroid receptor heterodimerization demonstrated in vitro and in vivo. *Proc Natl Acad Sci U S A* **92**, 12480-12484 (1995).
25. M. Nishi, M. Tanaka, K. Matsuda, M. Sunaguchi, M. Kawata, Visualization of glucocorticoid receptor and mineralocorticoid receptor interactions in living cells with GFP-based fluorescence resonance energy transfer. *J Neurosci* **24**, 4918-4927 (2004).
26. J. R. Pooley *et al.*, Beyond the heterodimer model for mineralocorticoid and glucocorticoid receptor interactions in nuclei and at DNA. *PLoS One* **15**, e0227520 (2020).
27. C. A. Rivers *et al.*, Glucocorticoid Receptor-Tethered Mineralocorticoid Receptors Increase Glucocorticoid-Induced Transcriptional Responses. *Endocrinology* **160**, 1044-1056 (2019).
28. T. Trapp, R. Rupprecht, M. Castren, J. M. Reul, F. Holsboer, Heterodimerization between mineralocorticoid and glucocorticoid receptor: a new principle of glucocorticoid action in the CNS. *Neuron* **13**, 1457-1462 (1994).
29. A. Jimenez-Panizo *et al.*, The multivalency of the glucocorticoid receptor ligand-binding domain explains its manifold physiological activities. *Nucleic Acids Res* **50**, 13063-13082 (2022).
30. V. Paakinaho, T. A. Johnson, D. M. Presman, G. L. Hager, Glucocorticoid receptor quaternary structure drives chromatin occupancy and transcriptional outcome. *Genome Res* **29**, 1223-1234 (2019).
31. D. M. Presman *et al.*, DNA binding triggers tetramerization of the glucocorticoid receptor in live cells. *Proc Natl Acad Sci U S A* **113**, 8236-8241 (2016).
32. D. M. Presman, G. L. Hager, More than meets the dimer: What is the quaternary structure of the glucocorticoid receptor? *Transcription* **8**, 32-39 (2017).
33. M. A. Digman, R. Dalal, A. F. Horwitz, E. Gratton, Mapping the number of molecules and brightness in the laser scanning microscope. *Biophys J* **94**, 2320-2332 (2008).
34. D. M. Presman *et al.*, Live cell imaging unveils multiple domain requirements for in vivo dimerization of the glucocorticoid receptor. *PLoS Biol* **12**, e1001813 (2014).
35. P. Fuentes-Prior, A. Rojas, A. T. Hagler, E. Estebanez-Perpina, Diversity of Quaternary Structures Regulates Nuclear Receptor Activities. *Trends Biochem Sci* **44**, 2-6 (2019).
36. J. G. McNally, W. G. Muller, D. Walker, R. Wolford, G. L. Hager, The glucocorticoid receptor: rapid exchange with regulatory sites in living cells. *Science* **287**, 1262-1265 (2000).
37. G. Fejes-Toth, D. Pearce, A. Naray-Fejes-Toth, Subcellular localization of mineralocorticoid receptors in living cells: effects of receptor agonists and antagonists. *Proc Natl Acad Sci U S A* **95**, 2973-2978 (1998).
38. R. F. Walther *et al.*, A serine/threonine-rich motif is one of three nuclear localization signals that determine unidirectional transport of the mineralocorticoid receptor to the nucleus. *J Biol Chem* **280**, 17549-17561 (2005).
39. M. Lombes, S. Kenouch, A. Souque, N. Farman, M. E. Rafestin-Oblin, The mineralocorticoid receptor discriminates aldosterone from glucocorticoids independently of the 11 beta-hydroxysteroid dehydrogenase. *Endocrinology* **135**, 834-840 (1994).
40. F. L. Groeneweg *et al.*, Quantitation of glucocorticoid receptor DNA-binding dynamics by single-molecule microscopy and FRAP. *PLoS One* **9**, e90532 (2014).
41. L. Amazit *et al.*, Finerenone Impedes Aldosterone-dependent Nuclear Import of the Mineralocorticoid Receptor and Prevents Genomic Recruitment of Steroid Receptor Coactivator-1. *J Biol Chem* **290**, 21876-21889 (2015).
42. B. Gravez *et al.*, The diuretic torasemide does not prevent aldosterone-mediated mineralocorticoid receptor activation in cardiomyocytes. *PLoS One* **8**, e73737 (2013).
43. J. T. Bridgham, S. M. Carroll, J. W. Thornton, Evolution of hormone-receptor complexity by molecular exploitation. *Science* **312**, 97-101 (2006).
44. T. J. Cole *et al.*, Aldosterone-Mediated Renal Sodium Transport Requires Intact Mineralocorticoid Receptor DNA-Binding in the Mouse. *Endocrinology* **156**, 2958-2968 (2015).
45. D. Pearce, A. Naray-Fejes-Toth, G. Fejes-Toth, Determinants of subnuclear organization of mineralocorticoid receptor characterized through analysis of wild type and mutant receptors. *J Biol Chem* **277**, 1451-1456 (2002).
46. K. Dahlman-Wright, A. Wright, J. A. Gustafsson, J. Carlstedt-Duke, Interaction of the glucocorticoid receptor DNA-binding domain with DNA as a dimer is mediated by a short segment of five amino acids. *J Biol Chem* **266**, 3107-3112 (1991).

47. C. M. Jewell, A. B. Scoltock, B. L. Hamel, M. R. Yudt, J. A. Cidlowski, Complex human glucocorticoid receptor dim mutations define glucocorticoid induced apoptotic resistance in bone cells. *Mol Endocrinol* **26**, 244-256 (2012).
48. T. A. Johnson, V. Paakinaho, S. Kim, G. L. Hager, D. M. Presman, Genome-wide binding potential and regulatory activity of the glucocorticoid receptor's monomeric and dimeric forms. *Nat Commun* **12**, 1987 (2021).
49. X. Liu *et al.*, Disruption of a key ligand-H-bond network drives dissociative properties in vamorolone for Duchenne muscular dystrophy treatment. *Proc Natl Acad Sci U S A* **117**, 24285-24293 (2020).
50. J. B. Pippal, Y. Yao, F. M. Rogerson, P. J. Fuller, Structural and functional characterization of the interdomain interaction in the mineralocorticoid receptor. *Mol Endocrinol* **23**, 1360-1370 (2009).
51. C. Hellal-Levy *et al.*, Specific hydroxylations determine selective corticosteroid recognition by human glucocorticoid and mineralocorticoid receptors. *FEBS Lett* **464**, 9-13 (1999).
52. J. Echave, C. O. Wilke, Biophysical Models of Protein Evolution: Understanding the Patterns of Evolutionary Sequence Divergence. *Annu Rev Biophys* **46**, 85-103 (2017).
53. M. S. Fornasari, G. Parisi, J. Echave, Quaternary structure constraints on evolutionary sequence divergence. *Mol Biol Evol* **24**, 349-351 (2007).
54. J. A. Marsh, S. A. Teichmann, Structure, dynamics, assembly, and evolution of protein complexes. *Annu Rev Biochem* **84**, 551-575 (2015).
55. E. D. Levy, E. Boeri Erba, C. V. Robinson, S. A. Teichmann, Assembly reflects evolution of protein complexes. *Nature* **453**, 1262-1265 (2008).
56. D. Odokonyero *et al.*, Loss of quaternary structure is associated with rapid sequence divergence in the OSBS family. *Proc Natl Acad Sci U S A* **111**, 8535-8540 (2014).
57. M. H. Ali, B. Imperiali, Protein oligomerization: how and why. *Bioorg Med Chem* **13**, 5013-5020 (2005).
58. K. De Bosscher, S. J. Desmet, D. Clarisse, E. Estebanez-Perpina, L. Brunsveld, Nuclear receptor crosstalk - defining the mechanisms for therapeutic innovation. *Nat Rev Endocrinol* **16**, 363-377 (2020).
59. M. F. Ogara *et al.*, The glucocorticoid receptor interferes with progesterone receptor-dependent genomic regulation in breast cancer cells. *Nucleic Acids Res* **47**, 10645-10661 (2019).
60. K. Barrett Mueller *et al.*, Estrogen receptor inhibits mineralocorticoid receptor transcriptional regulatory function. *Endocrinology* **155**, 4461-4472 (2014).
61. P. Kiilerich *et al.*, Interaction between the trout mineralocorticoid and glucocorticoid receptors in vitro. *J Mol Endocrinol* **55**, 55-68 (2015).
62. K. R. Mifsud, J. M. Reul, Acute stress enhances heterodimerization and binding of corticosteroid receptors at glucocorticoid target genes in the hippocampus. *Proc Natl Acad Sci U S A* **113**, 11336-11341 (2016).
63. X. M. Ou, J. M. Storring, N. Kushwaha, P. R. Albert, Heterodimerization of mineralocorticoid and glucocorticoid receptors at a novel negative response element of the 5-HT1A receptor gene. *J Biol Chem* **276**, 14299-14307 (2001).
64. M. Tsugita *et al.*, Glucocorticoid receptor plays an indispensable role in mineralocorticoid receptor-dependent transcription in GR-deficient BE(2)C and T84 cells in vitro. *Mol Cell Endocrinol* **302**, 18-25 (2009).
65. J. A. Marsh, S. A. Teichmann, Parallel dynamics and evolution: Protein conformational fluctuations and assembly reflect evolutionary changes in sequence and structure. *Bioessays* **36**, 209-218 (2014).
66. T. Perica, C. Chothia, S. A. Teichmann, Evolution of oligomeric state through geometric coupling of protein interfaces. *Proc Natl Acad Sci U S A* **109**, 8127-8132 (2012).
67. C. Aguilar-Sanchez *et al.*, Identification of permissive insertion sites for generating functional fluorescent mineralocorticoid receptors. *Endocrinology* **153**, 3517-3525 (2012).
68. S. H. Meijsing, C. Elbi, H. F. Luecke, G. L. Hager, K. R. Yamamoto, The ligand binding domain controls glucocorticoid receptor dynamics independent of ligand release. *Mol Cell Biol* **27**, 2442-2451 (2007).
69. S. Mikuni, M. Tamura, M. Kinjo, Analysis of intranuclear binding process of glucocorticoid receptor using fluorescence correlation spectroscopy. *FEBS Lett* **581**, 389-393 (2007).
70. F. Sievers *et al.*, Fast, scalable generation of high-quality protein multiple sequence alignments using Clustal Omega. *Mol Syst Biol* **7**, 539 (2011).

## SUPPLEMENTARY FIGURE LEGENDS

**Supplementary Figure S1**. (A) Representative image and molecular brightness (ε) in the nucleoplasm of cells stably expressing eGFP-tagged mouse MR (MR). We were unable to record from the MMTV array due to low levels of receptor expression. Individual dots represent values from one cell (n = 490, 307, 5; N.D., not determined). (B) Representative image and molecular brightness (ε) obtained from cells expressing eGFP-tagged wild type mouse GR (GR) and treated with 10 nM aldosterone for 1h (n = 490, 307, 15, 6). White arrows point to the MMTV array. Scale bars: 5 µm. To facilitate comparison, data from Fig.1 showing ε for GR-N525 in the nucleoplasm and MMTV array are shown.

**Supplementary Figure S2**. (A) Sequence comparison between mouse GR and MR DBDs. Highlighted residues were mutated during this study. (B) Schematic representation of mouse GR and MR DBDs, indicating key residues mutated in MR during this work. (C) Sequence comparison between mouse GR and MR LBDs. Residues GR-I634, part of an LBD-LBD dimerization interface (8) and conservative change MR-V830 are highlighted. Alignments were performed using Clustal Omega (70) and sequences with GenBank accesion numbers AAI29913 and AAI33714 for GR and MR, respectively.

**Supplementary Figure S3**. RT-qPCR performed on three MR up-regulated genes in cells expressing wild type MR or MR mutant P656R. Cells were treated with vehicle, with 10 nM aldosterone or 100 nM corticosterone for 2h. Plots show fold changes in the indicated nascent mRNA abundance compared to MR-P656R treated with vehicle (n = 2).